JPEDAV (2015) 36:544–553
DOI: 10.1007/s11669-015-0409-z
1547-7037 ©ASM International

Amendment of the Li-Bi Phase Diagram Crystal and Electronic Structure of Li_2Bi

Volodymyr Pavlyuk, Martyn Sozanskyi, Grygoriy Dmytriv, Sylvio Indris, and Helmut Ehrenberg

(Submitted June 13, 2015; in revised form September 5, 2015; published online September 21, 2015)

The phase diagram of the Li-Bi binary system was amended by x-ray analysis and differential scanning calorimetry. The formation of the binary compound Li_2Bi was confirmed and its structure determined by x-ray single crystal diffraction. The Li_2Bi compound crystallizes with the Mg_2Ga structure type (space group *P-62c*, hP18, a = 8.0712(4) Å, c = 6.8352(3) Å). The analysis of the interatomic distances together with electronic structure calculations using the tight-binding linear muffin-tin orbital atomic spheres approximations (TB-LMTO-ASA) indicate the dominance of a metallic type of bonding, although there is a weak partially ionic bonding, caused by charge transfer from Li to Bi.

Keywords binary diagram, crystal structure, intermetallics

1. Introduction

The binary, ternary and multicomponent lithium alloys and intermetallic compounds have been extensively studied in different fields and applications, including electrode materials for lithium-ion batteries, hydrogen storage materials, lightweight alloys and others.[1-12] In spite of intensive studies on lithium-containing binary systems, not all equilibrium phases are known yet. The Li-Zn[13,14] and the Li-In[15] systems are two examples with new binary phases established recently. The phase diagram of the system Li-Bi was first investigated by Grube et al.,[16] mainly based on thermal analysis and electrical resistivity measurements. The LiBi and Li_3Bi compounds were identified by Zintl and Brauer,[17] and their crystal structures were determined by x-ray diffraction.

The peritectic melting and polymorphic transformation of LiBi was also confirmed by Weppner and Huggins.[18] The Li_3Bi phase melts congruently and was later also prepared as solid films by the direct reaction of Bi(s) and Li(g) at low pressure and 200 °C.[19] The thermodynamic properties of Li-Bi alloys are described in references.[18,20-23] The assessed Li-Bi phase diagram is based on data from Sangster and Pelton[24] and shown in Fig. 1(a).

Volodymyr Pavlyuk, Department of Inorganic Chemistry, Ivan Franko Lviv National University, Kyryla and Mefodiya Str., 6, Lviv 79005, Ukraine and Institute of Chemistry, Environment Protection and Biotechnology, Jan Dlugosz University, Al. Armii Krajowej 13/15, 42-200 Czestochowa, Poland; **Martyn Sozanskyi** and **Grygoriy Dmytriv**, Department of Inorganic Chemistry, Ivan Franko Lviv National University, Kyryla and Mefodiya str., 6, 79005, Lviv, Ukraine; and **Sylvio Indris** and **Helmut Ehrenberg**, Karlsruhe Institute of Technology (KIT), Institute for Applied Materials (IAM), Hermann-von-Helmholtz-Platz 1, 76344 Eggenstein-Leopoldshafen, Germany. Contact e-mail: vpavlyuk2002@yahoo.com.

The thin films of Li-Bi alloys were prepared by Hiratani et al.[25] It was found that a new compound Li_2Bi was formed in addition to two known intermetallic compounds, LiBi and Li_3Bi. The x-ray diffraction patterns after heat treatment showed that this new compound was frozen in a meta-stable state at room temperature.

This paper includes new results on the Li-Bi phase diagram. The synthesis and crystal structure of the binary phase Li_2Bi are described.

2. Experimental Details

Lithium and bismuth, all with a nominal purity higher than 99.9% w/w, were used as starting materials for syntheses of $Li_{75}Bi_{25}$, $Li_{66.7}Bi_{33.3}$ and $Li_{50}Bi_{50}$ binary alloys. All preparation steps were performed in a glove box under dried argon atmosphere. The melting of the metals was carried out within sealed tantalum crucibles in an induction furnace at 1100 °C. After 10 min, the sample was rapidly cooled down to room temperature by removing the crucible from the furnace. After thermal treatment at 200 °C during 400 h, the sample could easily be separated from the opened tantalum container. No side-reaction of the alloy with the crucible was detected. The brittle dark-gray metallic alloys are very sensitive to the humidity in air. The amount of Li-loss during sample preparation in hermetically closed crucibles can be estimated, based on previous studies with successive detailed chemical analyses of similar systems.[6-8,26] Accordingly, a lithium loss up to 1% versus the nominal composition can be expected. In addition, for the alloys the content of lithium was determined by means of Flapho-4 flame photometer (Carl Zeiss Jena) with interference filter (671 nm).

X-ray powder diffraction of the samples was carried out using a STOE STADI/P powder diffractometer (Mo $K\alpha_1$-radiation, step scanning). Rietveld refinements, based on x-ray powder diffraction data (XRPD), were performed with the FULLPROF program.[27]

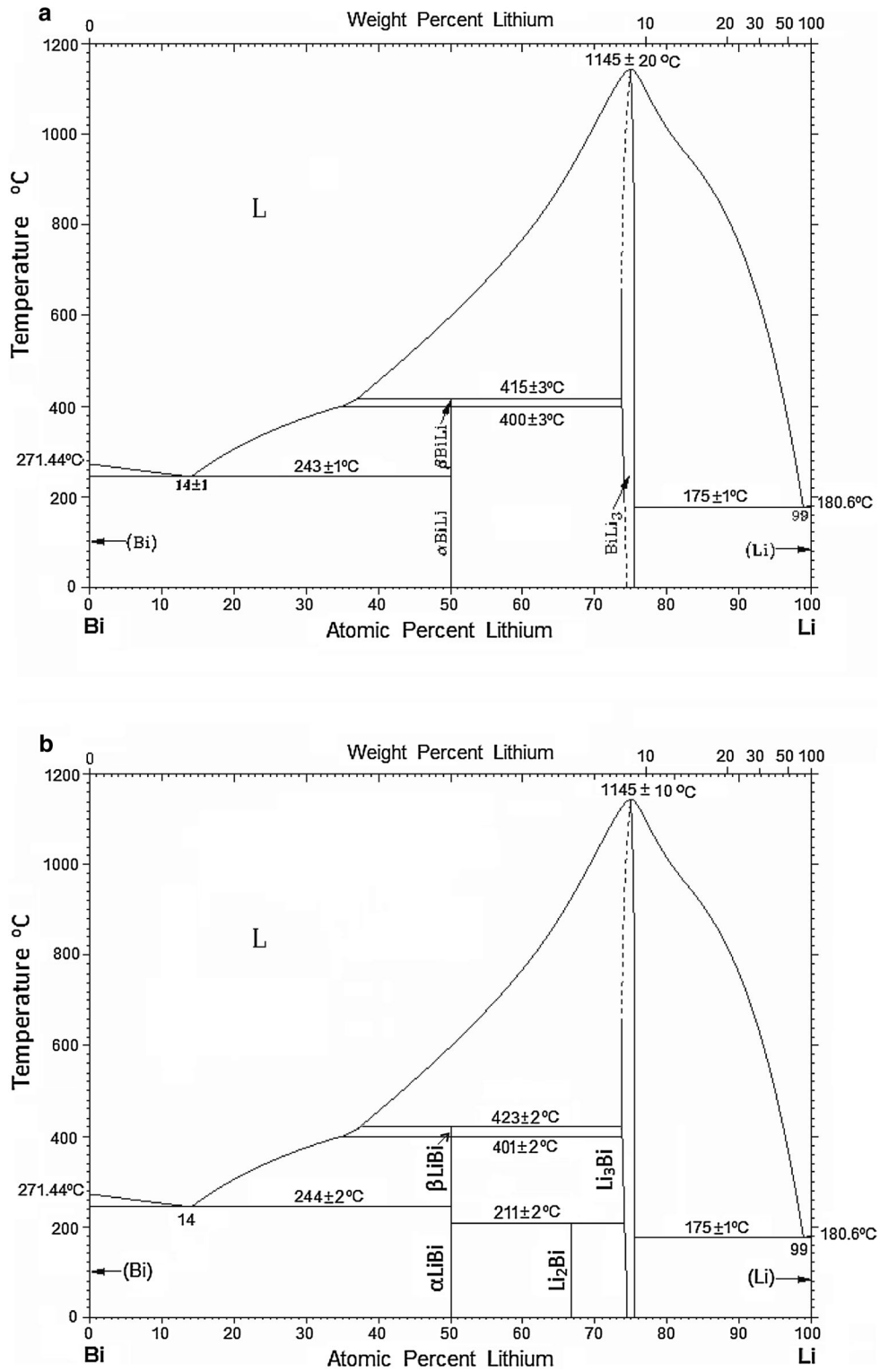

Fig. 1 The phase diagram of Li-Bi system redrawn from[27] (a) and amendment (b)

X-ray singe crystal diffraction was used for detailed crystal structure refinements. The intensity data were collected by an automatic four-circle diffractometer Xcalibur from Oxford Diffraction, equipped with CCD detector and graphite- monochromatized Mo Kα radiation. Scans were taken in ω mode, and CrysalisRed[28] was used for

Table 1 Nominal composition, XRPD and flame photometry data on selected Li-Bi as cast and annealed at 200 °C alloys

Nominal composition	Cast alloys		Annealed alloys	
	Compositions of alloy by flame photometry (at.%)	Phases content (%) by XRPD	Compositions of alloy by flame photometry (at.%)	Phases content (%) by XRPD
$Li_{75}Bi_{25}$	$Li_{75.3}Bi_{24.7}$	Li_3Bi (100)	$Li_{74.3}Bi_{25.7}$	Li_3Bi (100)
$Li_{66.7}Bi_{33.3}$	$Li_{68.7}Bi_{31.3}$	Li_2Bi (18)	$Li_{68.1}Bi_{31.9}$	Li_2Bi (47)
		LiBi (34)		LiBi (32)
		Li_3Bi (48)		Li_3Bi (21)
$Li_{50}Bi_{50}$	$Li_{50.8}Bi_{49.2}$	LiBi (82)	$Li_{49.6}Bi_{50.4}$	LiBi (95)
		Li_2Bi (7)		Li_2Bi (5)
		Li_3Bi (11)		

Table 2 Li-Bi solid phases

Phase	Entry prototype/Pearson symbol	SG symbol	Lattice parameters, Å		*T*, °C	Reaction type
			a	*c*		
Li	W, *cI2*	*Im-3 m*	3.5130(1)[37]	…	180.6	Melting
Li_3Bi	BiF_3, *cF16*	*Fm-3 m*	**6.7063(2)**	…	**1145 (10)**	Congruent
			6.708[17]	…	1145[24]	L ⇌ Li_3Bi
Li_2Bi	**Mg_2Ga, *hP18***	***P-62c***	**8.0712(4)***	**6.8352(3)***	**211(2)**	**Peritectoid**
	Mg_2In, *hP9*	*P-62 m*	8.054[25]	3.427[25]		Li_3Bi +LiBi ⇌ Li_2Bi
α-LiBi	AuCu, *tP2*	*P4/mmm*	**3.36104(3)**	**4.24404(6)**	**401(2)**	Polymorphic transformation
			3.361[17]	4.247[17]	400[16]	α-LiBi ⇌ β-LiBi
β-LiBi	…	…	…	…	**423(2)**	Peritectic
					415[16]	L + Li_3Bi ⇌ LiBi
Bi	As, *hR6*	*R-3 m*	4.3532(1)[37]	11.8147(2)[37]	271.4	Melting

In bold—experimental data specified in this work

* Single crystal data

analytical absorption corrections. The crystal structure was solved by direct methods and refined using the SHELX-97 program package.[29,30]

The electronic structures of the compounds were calculated using the tight-binding linear muffin-tin orbital (TB-LMTO) method in the atomic spheres approximation (TB-LMTO-ASA,[31-33] using the experimental crystallographic data reported here. The exchange and correlation were interpreted in the local density approximation.[34] All the figures and graphics concerning electron structure calculations were generated using wxDragon.[35]

The thermal DSC-TG-DTG analysis was carried out with the NETZSCH STA-449 simultaneous thermal analyzer. Samples of approximately 0.030 g were heated in corundum crucibles. The heating was performed under static conditions in argon atmosphere in the range of 30-600 °C with the temperature rate increase of 5 K/min. They provided the 0.5 °C precision in reading of temperature.

Both ^{6}Li and ^{7}Li nuclear magnetic resonance (NMR) spectroscopy has been extensively applied on inorganic and intermetallic lithium-containing compounds. The ^{6}Li isotope has as smaller nucler spin (I = 1), a smaller magnetogyric ratio, and a much smaller nuclear quadrupole moment. Therefore, sharp linewidths are achieved compared to the ^{7}Li isotope. Thus, ^{6}Li NMR was used to get a better resolution in the spectrum. The ^{6}Li magic angle spinning (MAS) NMR spectra were recorded with 2.5 mm zirconia rotors at room temperature with a single-pulse sequence, a RF pulse length of 2 μs, and a rotation frequency of 5 kHz. Chemical shifts are given relative to that of an aqueous 1 M ^{6}LiCl solution.

3. Results and Discussion

3.1 Phase Diagram of Li-Bi System

A re-examination of the Li-Bi system, based on differential scanning calorimetry, x-ray diffraction analysis and flame photometry of binary alloys (Tables 1, 2), revealed a more complex phase diagram in the composition range between LiBi and Li_3Bi than originally reported (Fig. 1b). The XRPD phase analysis shows that $Li_{75}Bi_{25}$ cast alloy is single-phase with cubic BiF_3 structure type. The $Li_{50}Bi_{50}$ cast alloy as a main phase consists of a tetragonal LiBi (AuCu structure type) and two Li_2Bi and

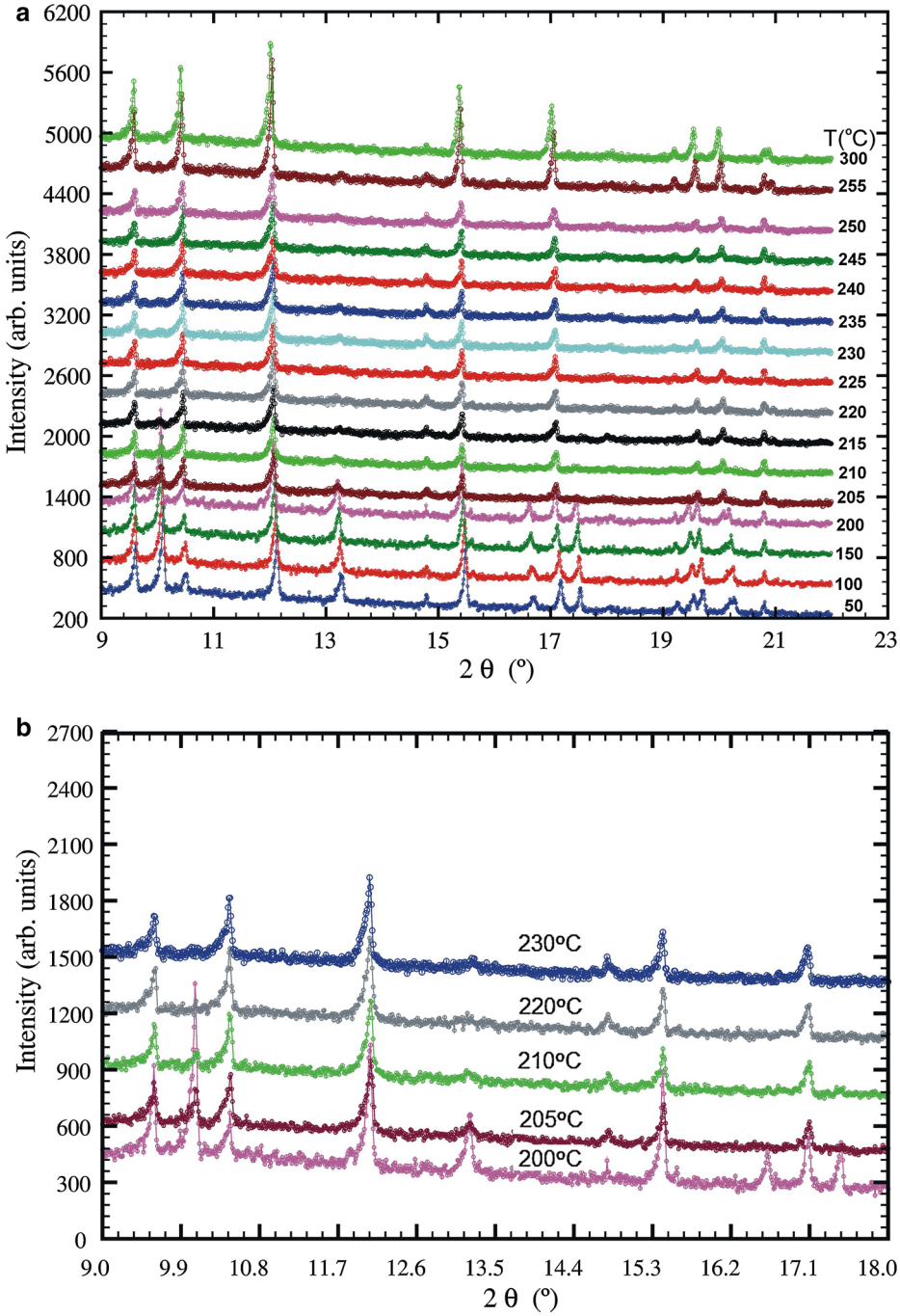

Fig. 2 Observed x-ray powder diffraction patterns in temperature range 50-300 °C (a) and selected powder patterns between 200 and 230 °C (b)

Li_3Bi additional phases the content of which was significantly reduced after annealing. Even after annealing the $Li_{66.7}Bi_{33.3}$ alloy was three-phase, and the content of the main Li_2Bi hexagonal phase was less than 50%. This is caused by such conditions as low temperature (200 °C) at which the process of phase formation in solid state cannot proceed rapidly. Good correlation between starting nominal composition and lithium content obtained by flame photometry for $Li_{75}Bi_{25}$ and $Li_{50}Bi_{50}$ annealed alloys is observed (Table 1). The difference between nominal composition and composition obtained by flame photometry is slightly higher for three phase $Li_{66.7}Bi_{33.3}$ alloy. The presence of Li_2Bi hexagonal phase in cast alloys and increase in the content of the annealed alloys suggest that it is the stable phase in contrast to results of the authors,[28] who observed this compound in thin films of Li-Bi alloys as a meta-stable phase. This compound forms at 211 °C by peritectoid reaction:

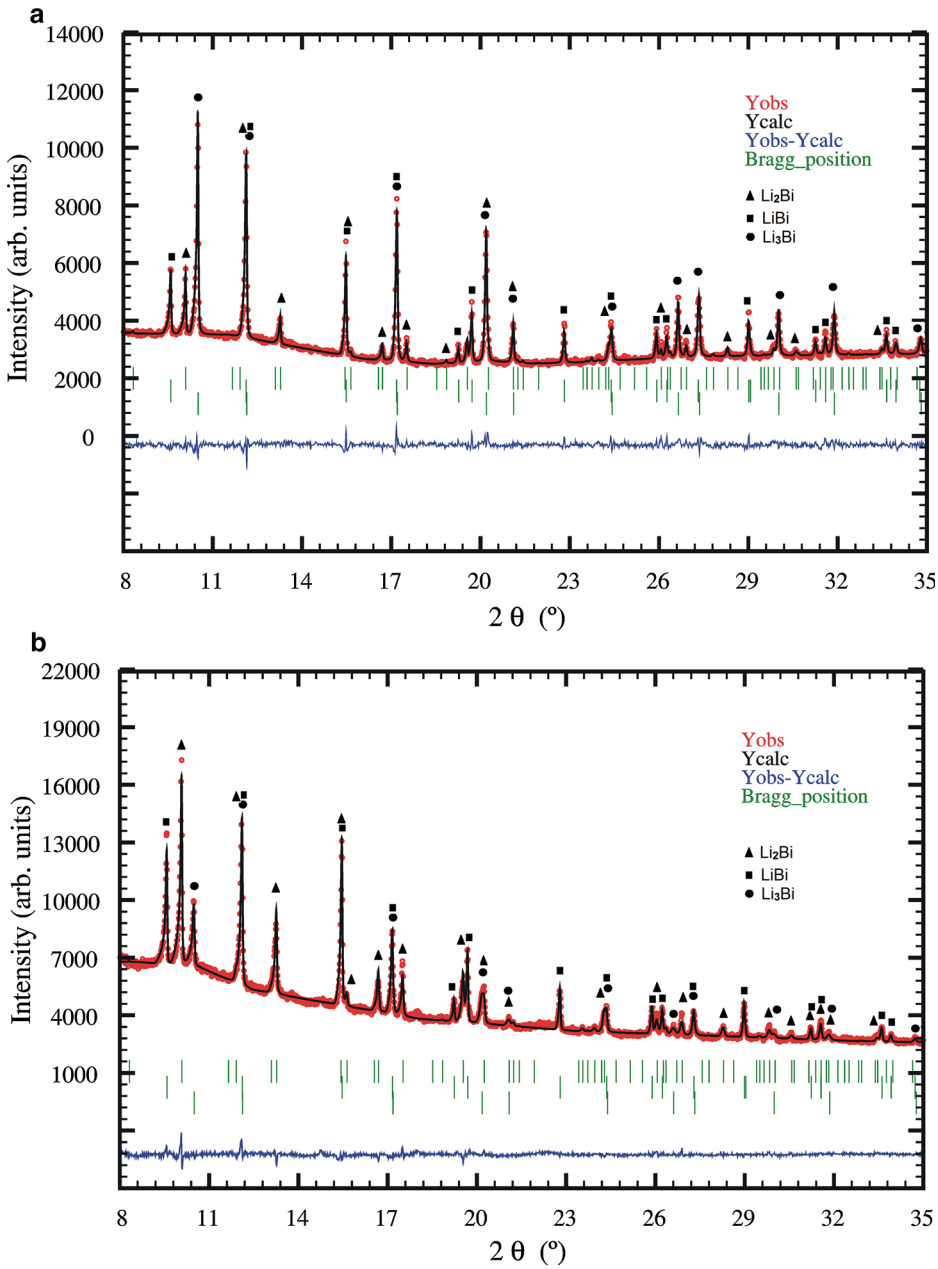

Fig. 3 Observed (red circles), calculated (black line) and difference (bottom blue line) x-ray powder diffraction patterns for $Li_{66.7}Bi_{33.3}$ as cast alloy (a) and annealed at 200 °C (b). Vertical bars indicate the Bragg positions of the corresponding phases. Symbols for phase identification: ▲—Li_2Bi, ■—LiBi and ●—Li_3Bi (Color figure online)

$$Li_3Bi + LiBi \rightleftharpoons Li_2Bi.$$

Powder patterns from a Li_2Bi alloy, measured sequentially with increasing temperature show that the hexagonal phase exists from room temperature up to 211 °C (Fig. 2). Above this temperature all powder patterns reflected only the coexistence of the tetragonal LiBi and the cubic Li_3Bi phases. The results of the Rietveld refinements of the as cast and annealed at 200 °C Li_2Bi alloy are shown Fig. 3. In addition to the reflections from the new hexagonal phase reflections from the known cubic and tetragonal phases are detected. The annealing of this alloy during 400 h at 200 °C increase the Li_2Bi phase content from 18% (for cast alloy) up to 47%. Subsequent continuation of annealing slightly increases the content of this phase. Differential scanning calorimetry determined the accurate temperature of the peritectoid reaction at 211 °C (Fig. 4).

For the already known phases Li_3Bi and LiBi congruent and peritectic reactions with the liquid melt (L) were confirmed at temperatures of 1145 and 423 °C, respectively:

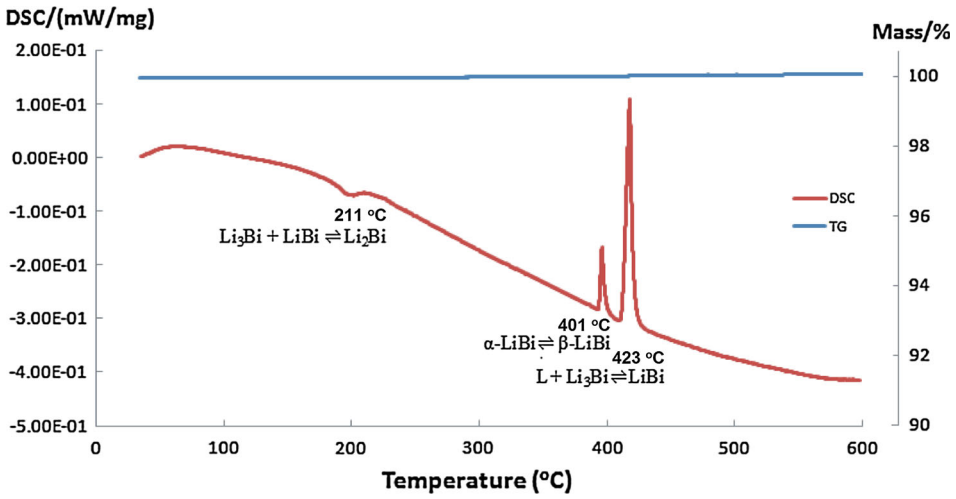

Fig. 4 DSC and TG curves for Li_2Bi sample at the cooling

Table 3 Crystal data and structure refinement

Empirical formula	Li_2Bi
Formula weight	222.86
Temperature	T = 293 K
Wavelength	Mo Kα, 0.71073 nm
Crystal system, space group	hexagonal, *P*-62*c* (190)
Pearson symbol, *Z*	*hP*18, 6
Crystal dimensions (mm^3)	0.02×0.03×0.08
Unit cell dimensions	a = 8.0712(4) Å
	c = 6.8352(3) Å
Volume	385.62 (3) $Å^3$
Calculated density	5.758 g/cm^3
Absorption coefficient	68.16 mm^{-1}
F(000)	534
Scan mode	ω
Theta range for data collection	θ_{max} = 27.2°, θ_{min} = 2.9°
Index ranges	$-5 \le h \le 5$, $-10 \le k \le 10$, $-8 \le l \le 8$
Reflections collected/unique	1284/322
Refinement method	Refinement on F^2
	Least-squares matrix: full
Weighting scheme	$w = 1/[\sigma^2(F_o^2) + (0.010P)^2]$ where $P = (F_o^2 + 2F_c^2)/3$
Data/parameters	322/13
Goodness of fit on F^2	0.92
$R[F^2 > 2\sigma(F^2)]$	0.023
$wR(F^2)$	0.102
Largest diff. peak and hole	1.34 and −1.79 e/$Å^3$

$$L \rightleftharpoons Li_3Bi$$

$$L + Li_3Bi \rightleftharpoons LiBi$$

For the equiatomic LiBi phase Grube et al.[16] observed two invariant reactions at 415 and 400 °C, assigned to the peritectic melting of LiBi and the polymorphic transformation α-LiBi ⇌ β-LiBi, respectively. According to our DSC data these temperature are 423 and 401 °C respectively. The tetragonal structure (AuCu structure type, *P*4/*mmm*) of the low temperature modification α-LiBi was confirmed in this study and more precise unit cell parameters could be refined: a = 3.36104(3), c = 4.24404(6) Å. The refined lattice parameter for cubic Li_3Bi (BiF_3 structure type, *Fm-3m*) at room temperature is a = 6.7063(2) Å. All known crystallographic data for solid phases in the Li-Bi system are summarized in Table 2, together with the types of reaction and the temperature of formation.

Table 4 Fractional atomic coordinates and isotropic or equivalent isotropic displacement parameters ($Å^2$) for Li_2Bi

Atoms	Site	*x*/*a*	*y*/*a*	*z*/*a*	U_{iso}*/U_{eq}	Occ.
Bi1	*4f*	1/3	2/3	0.03260(8)	0.0228 (3)	1
Bi2	*2b*	0	0	1/4	0.0210 (3)	1
Li1	*6h*	0.383(5)	0.376(4)	1/4	0.0301 (4)*	1
Li2	*6g*	0.289(4)	0	0	0.0310 (4)*	1

Atoms	U^{11}	U^{22}	U^{33}	U^{12}	U^{13}	U^{23}
Bi1	0.0228(4)	0.02283(4)	0.0228(5)	0.0114(2)	0.00000	0.00000
Bi2	0.0203(4)	0.0203(4)	0.0223(4)	0.0102(2)	0.00000	0.00000

3.2 Crystal and Electronic Structure of the Li_2Bi Binary Compound

From the annealed alloy of nominal composition $Li_{66.7}Bi_{33.3}$ a small prismatic single crystal was isolated by mechanical fragmentation. The structure solution by direct methods and subsequent structure refinement was performed using the SHELX97 software package. The structure was solved after an analytical absorption correction in the non-centrosymmetric space group *P*-62*c*, since the solution and refinement in centrosymmetric variants were not satisfactory. Selected information on single crystal x-ray data collection and refinements is given in Table 3, and the fractional atomic coordinates and thermal displacement parameters of the Li_2Bi compound are compiled in Table 4.

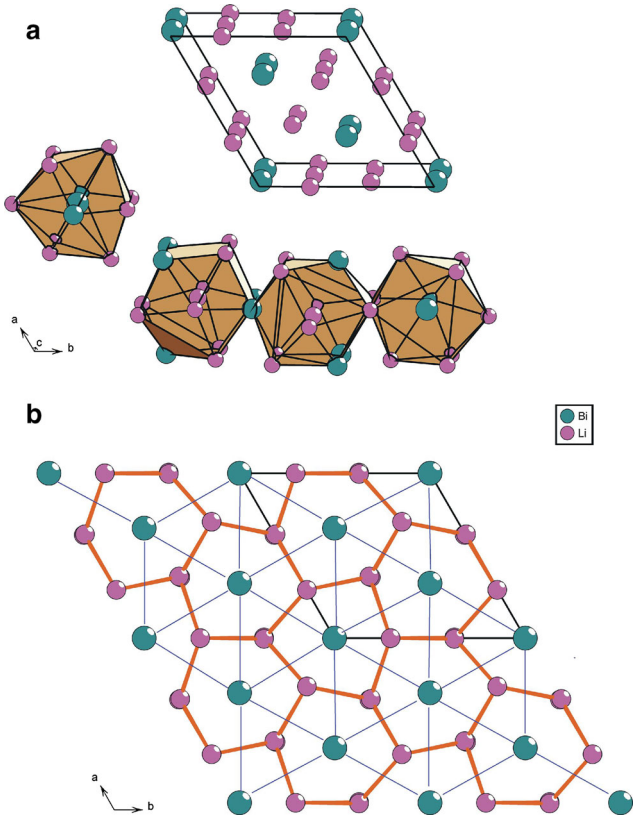

Fig. 5 Unit cell and coordination polyhedral of atoms (a) and atomic nets (b)

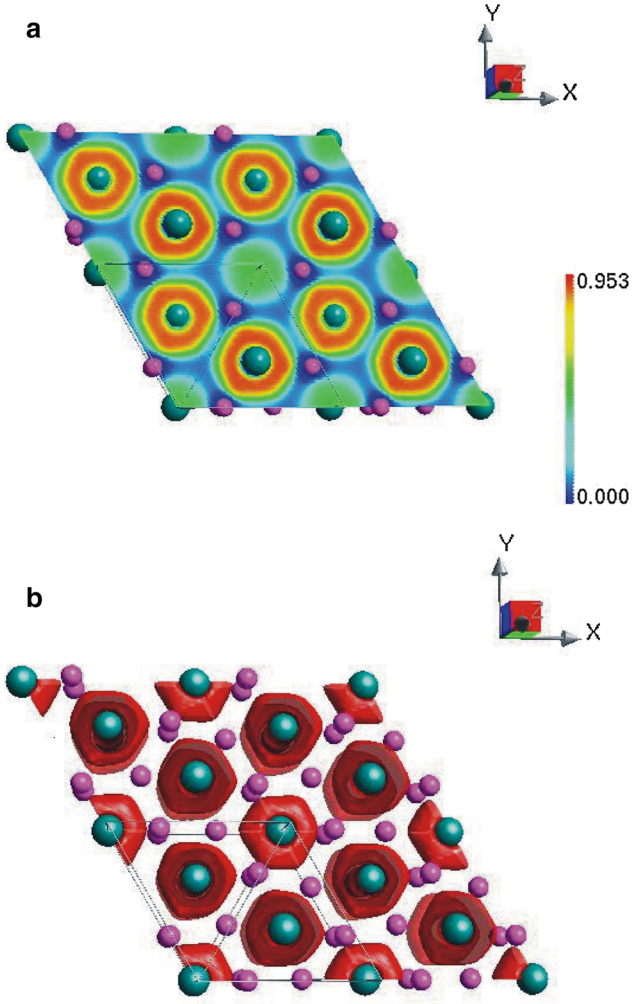

Fig. 6 The electron localization function (ELF) mapping (a) and isosurfaces (b) for Li_2Bi

The structure of title compound crystallizes in the Mg_2Ga-type.[36] Atoms of bismuth in the Li_2Bi structure occupy the *4f* and the *2b* sites, which are occupied by gallium atoms in Mg_2Ga. The lithium atoms occupy *6h* and *6g* sites as the magnesium atoms in Mg_2Ga. The unit cell of the Li_2Bi structure and the coordination polyhedra of all representative atoms are shown in Fig. 5(a). The coordination polyhedron of Li1 has 13 vertices and is a tricapped pentagonal prism [$Li1Bi_5Li_8$]. The coordination polyhedron of Li2 is an anticuboctahedron [$Li2Bi_4Li_8$]. For Bi1 the coordination polyhedron is a trigonal prism, in which the quadrilateral facets are centered by lithium atoms and the one base facet centered by a Bi atom [$Bi1Li_9Bi$]. Bi2 is surrounded by 11 atoms and the coordination polyhedra is a trigonal prism, in which the quadrilateral facets are centered by lithium and the two bases triangular facets by Bi atoms [$Bi2Li_9Bi_2$].

The crystal structure of Li_2Bi (Mg_2Ga-type) compound is also closely related to the Mg_2In (or Fe_2P) structure type which has a twice shorter unit cell dimension *c*. In this structure, both non-equivalent indium atoms have the same atomic coordination (c.n. = 11), while in the Li_2Bi compound the atoms of *p*-element (Bi) have different coordination numbers c.n. = 10 and c.n. = 11. This difference probably is the reason for doubling of unit cell dimension *c*.

At the refinement of the Li_2Bi in the Mg_2In (or Fe_2P) structure model proposed by Hiratani et al.[28] the *R*-factors are growing almost twice more ($R = 0.054$ in compare to $R = 0.023$ for Mg_2Ga type), and all refinement parameters are worse. Also our experimental data clearly shown that the model with *P-62c* space group is more correct, because the single crystal data consist enough visible reflexes which are absent in the model with *P-62m* space group, such as *011*, *013*, *023*, *−143* etc.

The structure of Li_2Bi (Fig. 5b) can be described by two different atomic networks: The lithium atoms form three-dimensional 6_3-nets with Bi atoms distributed in the hexagonal channels. Bismuth atoms form Kagome 3_6-nets.

Li_2Bi belongs to the 'classical' Zintl phases, because it contains an alkaline metal (Li) and a *p*-element (Bi), it is electronically balanced (lithium atoms form positively charged $2n[Li]^{\delta+}$ polycations, which compensate the negative charge of $n[Bi]^{2\delta-}$ polyanions) and has a very narrow or no homogeneity width (see phase diagram, Fig. 1). Electronic structure calculations using the TB-LMTO-ASA confirm the Zintl concept and a charge transfer from Li to Bi. The electron localization function (ELF) mapping and

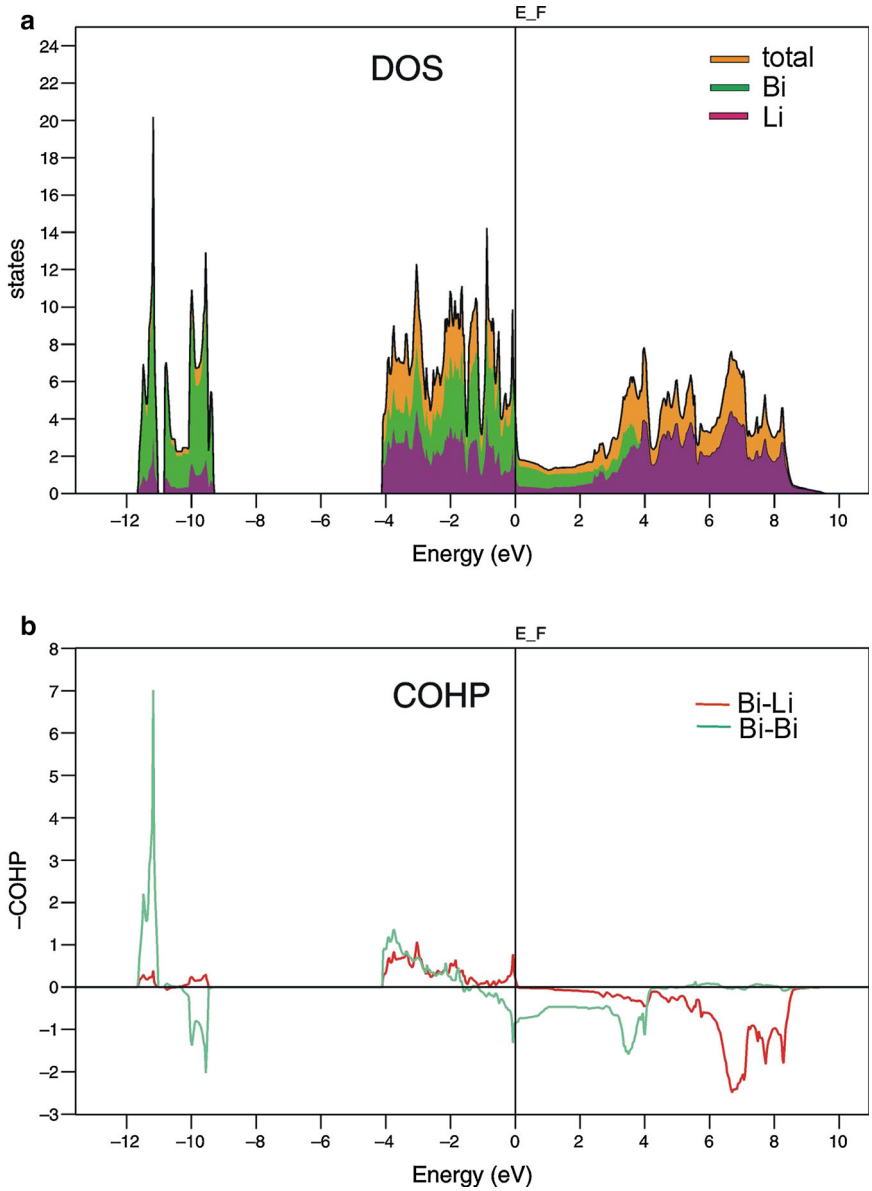

Fig. 7 Density of states (DOS) (a) and crystal orbital Hamilton populations (–COHP) per bond (b) for Li_2Bi from LMTO calculations

isosurfaces for Li_2Bi are shown in Fig. 6(a) and (b). Generally, in the case of a fully delocalized electron the ELF value is equal 0 and in the case of a fully localized electron equal 1. For the investigated phases the ELF is numerically bound between 0 (around Li) and 0.953 (around Bi). Thus, despite the partial ionization of all atoms, there are still sufficient delocalized electrons available that provide a dominant metallic bonding. A significant decrease of the density of states (DOS) at the Fermi level (Fig. 7a) indicates a semi-metallic behavior. Such a behavior is typical for Zintl phases, which are poor conductors or semiconductors.

The quantitative evaluation of the bonding strength between the different types of atoms in Li_2Bi was obtained from the crystal orbital Hamilton population (COHP) and integrated COHP (iCOHP) calculations (Fig. 7b; Table 4). From the COHP curves the strongest interactions are concluded between Bi-Bi atoms. The Bi1-Bi1 distance (2.9720 Å) is shorter than Bi2-Bi2 (3.4176 Å), indicating an increase of the bond strength and an increases of the -iCOHP parameter from 1.727 to 0.754 eV, respectively. The interactions between Li and Bi atoms are somewhat weaker and for the shortest distances within 0.363-0.585 eV (Table 5).

An analysis of the interatomic distances together with electronic structure calculations indicates the dominance of a metallic type of bonding, although there is also a weak partially ionic bonding, caused by charge transfer from Li to Bi.

The ^{6}Li MAS NMR spectrum of Li_2Bi (Fig. 8) is dominated by a main peak at +15.4 ppm. The large positive shift is a so-called Knight shift resulting from interaction of the Li nucleus with delocalized electrons, further confirming the metallic character of the sample. Some minor contribu-

Table 5 Interatomic distances (δ, Å) for Li_2Bi

Atoms	δ, Å	−iCOHP, eV	Atoms	δ, Å	−iCOHP, eV
Bi1			Bi2		
3Li2	2.8968(1)	0.585	6Li2	2.8884(1)	0.376
3Li1	2.9704(1)	0.363	3Li1	3.0611(2)	0.517
Bi1	2.9720(1)	1.727	2Bi2	3.4176(2)	0.754
3Li1	3.1432(1)	0.346	…	…	…
Bi1	3.8632(2)	0.048	…	…	…
Li1			Li2		
2Bi1	2.9704(1)	0.363	2Bi2	2.8884(1)	0.376
Bi2	3.0611(1)	0.517	2Bi1	2.8968(1)	0.585
2Bi1	3.1432(1)	0.346	2Li1	3.1803(1)	0.043
2Li2	3.1803(1)	0.043	2Li1	3.2224(1)	0.042
2Li2	3.2224(1)	0.042	2Li1	3.2844(1)	0.029
2Li2	3.2844(1)	0.029	2Li2	3.4176(2)	0.008
2Li1	3.4191(1)	0.018	…	…	…

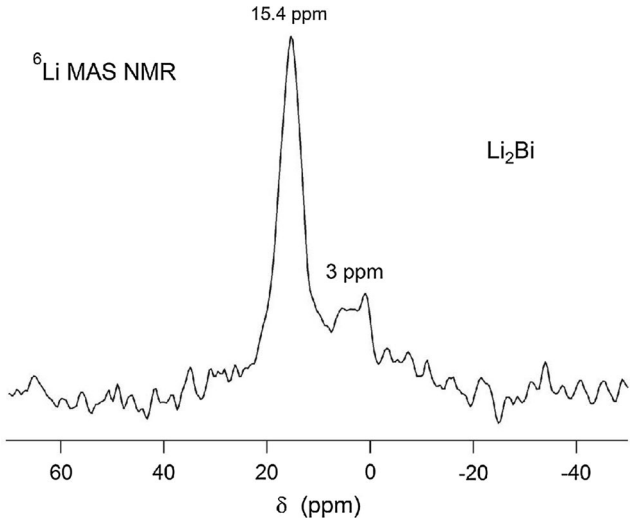

Fig. 8 The ^{6}Li MAS nuclear magnetic resonance (NMR) spectra for Li_2Bi

tion was observed at about 3 ppm, probably from an impurity phase or an interstitial Li site in the structure with very low occupation probability.

Acknowledgments

Financial support from the National Science Centre, Poland (No. 2014/15/B/ST8/00101) is gratefully acknowledged.

References

1. B. Scrosati and J. Garche, Lithium Batteries: Status, Prospects and Future, *J. Power Sources*, 2010, **195**, p 2419-2430
2. C.-M. Park, J.-H. Kim, H. Kim, and H.-J. Sohn, Li-Alloy Based Anode Materials for Li Secondary Batteries, *Chem. Soc. Rev.*, 2010, **39**, p 3115-3141
3. F. Thoss, L. Giebeler, S. Oswald, H. Ehrenberg, and J. Eckert, Study on the Reversible Li-Insertion of Amorphous and Partially Crystalline $Al_{86}Ni_8La_6$ and $Al_{86}Ni_8Y_6$ Alloys as Anode Materials for Li-Ion Batteries, *Electrochim. Acta*, 2012, **60**, p 85-94
4. I. Chumak, G. Dmytriv, V. Pavlyuk, S. Oswald, J. Eckert, H. Trill, and H. Eckert, Li(Al1-zZnz) Alloys as Anode Materials for Rechargeable Li-Ion Batteries, *J. Mater. Res.*, 2010, **25**, p 1492-1499
5. V. Pavlyuk, G. Dmytriv, I. Chumak, O. Gutfleisch, I. Lindemann, and H. Ehrenberg, High Hydrogen Content Super-Lightweight Intermetallics from the Li-Mg-Si System, *Int. J. Hydrogen Energy*, 2013, **38**, p 724-737
6. G. Dmytriv, H. Pauly, H. Ehrenberg, V. Pavlyuk, and E. Vollmar, Homogeneity Range of the NaTl-type Zintl Phase in the Ternary System Li-In-Ag, *J. Solid State Chem.*, 2005, **178**, p 2825-2831
7. V. Pavlyuk, G. Dmytriv, I. Chumak, H. Ehrenberg, and H. Pauly, The Crystal Structure of the $LiAg_2In$ Compound, *J. Solid State Chem.*, 2005, **178**, p 3303-3307
8. V. Pavlyuk, G. Dmytriv, I. Tarasiuk, H. Pauly, and H. Ehrenberg, The Ternary Indide Li278(In, Ag)154: A New n = 6 Variant of Cubic n×n×n W-Type Superstructures, *Intermetallics*, 2007, **15**, p 1409-1415
9. V. Pavlyuk, G. Dmytriv, I. Tarasiuk, I. Chumak, H. Pauly, and H. Ehrenberg, $Li_8Cu_{12+x}Al_{6-x}$ (x = 1.16): A New Structure Type Related to Laves Phases, *Acta Crysallogr.*, 2008, **C64**, p 15-17
10. V. Pavlyuk, G. Dmytriv, I. Tarasiuk, I. Chumak, H. Pauly, and H. Ehrenberg, $Li_{12}Cu_{16+x}Al_{26-x}$ (x = 3.2): A New Intermetallic Structure Type, *Acta Crysallogr.*, 2008, **C64**, p 73-75
11. V. Pavlyuk, G. Dmytriv, I. Tarasiuk, I. Chumak, H. Pauly, and H. Ehrenberg, Polymorphism of LiAg. Solid State, *Science*, 2010, **12**, p 274-280
12. G. Dmytriv, V. Pavlyuk, H. Pauly, J. Eckert, and H. Ehrenberg, New Real Ternary and Pseudoternary Phases in the Li-Au-In-System, *J. Solid State Chem.*, 2011, **184**, p 1328-1332
13. V. Pavlyuk, I. Chumak, and H. Ehrenberg, Polymorphism of Li_2Zn_3, *Acta Crysallogr.*, 2012, **B68**, p 34-39
14. V. Pavlyuk, I. Chumak, L. Akselrud, S. Lidin, and H. Ehrenberg, $LiZn_{4-x}$ (x = 0.825) as a (3 + 1)-Dimensional Modulated Derivative of Hexagonal Close Packing, *Acta Crysallogr.*, 2014, **B70**, p 212-217
15. V. Pavlyuk, I. Chumak, and H. Ehrenberg, Binary Lithium Indides $Li_{22-x}In_{8+x}$ (x = 0.1), $Li_{11-x}In_{4+x}$ (x = 1.05), and $Li_{10-x}In_{2+x}$ (x = 1.59) with Clusters, *Eur. J. Inorg. Chem.*, 2014, **12**, p 2053-2064
16. G. Grube, H. Vosskühler, and H. Schlecht, Electrical Conductivity and Phase Diagrams of Binary Alloys. 12. The Bi-Li System, *Z. Elektmchem.*, 1934, **40**, p 270-274
17. E. Zintl and G. Brauer, Metals and Alloys. 14. Constitution of Bi-Li Alloys, *Z. Elektmchem.*, 1935, **41**, p 297-303
18. W. Weppner and R.A. Huggins, Thermodynamic Properties of the Intermetallic Systems Li-Sb and Li-B, *J. Electrochem. Soc.*, 1978, **125**, p 7-14
19. R. Gobrecht, On Li Bismuthide, *Ann. Phys. Ser.*, 1967, **20**(5/6), p 262-264
20. W. Seith and O. Kubaschewski, The Heats of Formation of Several Alloys, *Z. Elektmchem.*, 1937, **43**, p 743-749
21. M.S. Foster, S.E. Wood, and C.E. Crouthamel, Thermodynamics of Binary Alloys. I. The Bi-Li System, *Inorg. Chem.*, 1964, **3**, p 1428-1431
22. B. Predel and G. Oehme, Calorimetric Study of Liquid Li-Tl, In-Li and Bi-Li Alloys, *Z. Metallkd.*, 1979, **70**, p 618-623

23. A. Neubert, H.R. Ihle, and K.A. Gingerich, Thermodynamic Study of the Molecules BiLi and PbLi by Knudsen Effusion Mass Spectrometry, *J. Chem. Phys.*, 1980, **73**, p 1406-1409
24. J. Sangster and A.D. Pelton, The Bi-Li (Bismuth-Lithium) System, *J. Phase Equilibria*, 1991, **12**, p 447-450
25. M. Hiratani, Y. Ito, K. Miyauchi, and T. Kudo, Thin Film Formation of Li-Bi Alloy and Identification of a New Intermetallic Compound, *Mater. Res. Bull.*, 1988, **23**, p 1739-1746
26. H. Pauly, A. Weiss, and H. Witte, The Crystal Structure of the Ternary Intermetallic Phases Li_2 EX (E = Cu, Ag, Au; X = Al, Ga, In, Tl, Si, Ge, Sn, Pb, Sb, Bi), *Z. Metallk.*, 1968, **59**, p 47-58
27. J. Rodriguez-Carvajal, Recent Advances in Magnetic Structure Determination by Neutron Powder Diffraction, *Physica B*, 1993, **192**, p 55-69
28. CrysAlis PRO Agilent, *CrysAlis PRO*, Agilent Technologies, Yarnton, 2011
29. G.M. Sheldrick, *SHELXS, Program for the Solution of Crystal Structures*, University of Goettingen, Goettingen, 1997
30. G.M. Sheldrick, *SHELXL-97, Program for Crystal Structure Refinement*, University of Goettingen, Goettingen, 1997
31. O.K. Andersen, Linear Methods in Band Theory, *Phys. Rev. B*, 1975, **12**, p 3060-3083
32. O.K. Andersen and O. Jepsen, Explicit, First-Principles Tight-Binding Theory, *Phys. Rev. Lett.*, 1984, **53**, p 2571-2574
33. O.K. Andersen, Z. Pawlowska, and O. Jepsen, Illustration of the Linear-Muffin-Tin-Orbital Tight-Binding Representation: Compact Orbitals and Charge Density in Si, *Phys. Rev. B*, 1986, **34**, p 51-53
34. U. von Barth and L. Hedin, A Local Exchange-Correlation Potential for the Spin Polarized Case, *I. J. Phys. C*, 1972, **5**, p 1629-1714
35. B. Eck, wxDragon 1.6.6, Aachen, 1994-2010, http://www.ssc.rwth-aachen.de, Accessed Apr 7, 2013
36. K. Frank and K. Schubert, Kristallstruktur von Mg_2Ga und Mg_2Tl, *J. Less Common Met.*, 1970, **20**, p 215-221
37. P. Villars and K. Cenzual, *Pearson's Crystal*, Version 1.0, Release 2007/8, ASM International, Materials Park